Monthly Notices
of the
ROYAL ASTRONOMICAL SOCIETY

MNRAS **428,** 3366–3374 (2013) doi:10.1093/mnras/sts279

On the role of feedback in shaping the cosmic abundance and clustering of neutral atomic hydrogen in galaxies

Han-Seek Kim,[1⋆] C. Power,[2,4⋆] C. M. Baugh,[3] J. S. B. Wyithe,[1,4] C. G. Lacey,[3] C. D. P. Lagos[3] and C. S. Frenk[3]

[1]*School of Physics, The University of Melbourne, Parkville, VIC 3010, Australia*
[2]*International Centre for Radio Astronomy Research, University of Western Australia, 35 Stirling Highway, Crawley, WA 6009, Australia*
[3]*Institute for Computational Cosmology, Department of Physics, University of Durham, South Road, Durham DH1 3LE*
[4]*ARC Centre of Excellence for All-Sky Astrophysics (CAASTRO)*

Accepted 2012 October 23. Received 2012 October 21; in original form 2012 August 13

ABSTRACT

We investigate the impact of feedback – from supernovae (SNe), active galactic nuclei (AGN) and a photoionizing background at high redshifts – on the neutral atomic hydrogen (H I) mass function, the b_J-band luminosity function, and the spatial clustering of these galaxies at $z = 0$. We use a version of the semi-analytical galaxy formation model GALFORM that calculates self-consistently the amount of H I in a galaxy as a function of cosmic time and links its star formation rate to its mass of molecular hydrogen (H_2). We find that a systematic increase or decrease in the strength of SN feedback leads to a systematic decrease or increase in the amplitudes of the luminosity and H I mass functions, but has little influence on their overall shapes. Varying the strength of AGN feedback influences only the numbers of the brightest or most H I massive galaxies, while the impact of varying the strength of photoionization feedback is restricted to changing the numbers of the faintest or least H I massive galaxies. Our results suggest that the H I mass function is a more sensitive probe of the consequences of cosmological reionization for galaxy formation than the luminosity function. We find that increasing the strength of any of the modes of feedback acts to weaken the clustering strength of galaxies, regardless of their H I richness. In contrast, weaker AGN feedback has little effect on the clustering strength, whereas weaker SN feedback increases the clustering strength of H I-poor galaxies more strongly than H I-rich galaxies. These results indicate that forthcoming H I surveys on next-generation radio telescopes such as the Square Kilometre Array and its pathfinders will be exploited most fruitfully as part of multiwavelength survey campaigns.

Key words: galaxies: formation – galaxies: luminosity function, mass function – large-scale structure of Universe – radio lines: galaxies.

1 INTRODUCTION

Neutral hydrogen, both atomic (H I) and molecular (H_2), plays a fundamental role in galaxy formation, principally as the raw material from which stars are made. The amount of neutral hydrogen in a galaxy at any given time reflects the complex interplay between processes that either deplete it, such as supernovae (SNe), or replenish it, such as gas cooling from hot atmospheres surrounding galaxies and by mergers with other gas-rich galaxies. By quantifying the properties of H I in galaxies and noting how these properties vary with galaxy morphology and environment, we can glean insights into the physics of galaxy formation and test predictions of theoretical models.

Most of what we know about the H I properties of galaxies comes from surveys of the nearby Universe ($z \lesssim 0.05$) such as H I Parkes All-Sky Survey (HIPASS; see Meyer et al. 2004) and Arecibo Legacy Fast ALFA Survey (ALFALFA; see Giovanelli et al. 2005). Such surveys have revealed that H I-rich galaxies tend to be late type (e.g. Kilborn et al. 2002; Evoli et al. 2011), but it is common for early-type field galaxies to host H I (e.g. Serra et al. 2012); that the H I mass function is well described by a Schechter function (e.g. Zwaan et al. 2003; Martin et al. 2010) but its shape depends on environment (e.g. Springob, Haynes & Giovanelli 2005; Zwaan et al. 2005; Kilborn et al. 2009); and that H I-rich galaxies are among the most weakly clustered galaxies known (e.g. Basilakos et al. 2007; Meyer et al. 2007; Passmoor, Cress & Faltenbacher 2011).

⋆E-mail: hansikk@unimelb.edu.au (H-SK); chris.power@icrar.org (CP)

However, knowledge of the H I properties of galaxies will improve many-fold over the coming decade with the advent of next-generation H I galaxy surveys on Australian Square Kilometre Array Pathfinder (ASKAP; cf. Johnston et al. 2008), Meer Karoo Array Telescope (MeerKAT; cf. Jonas 2007) and ultimately the Square Kilometre Array (SKA) itself (e.g. Baugh et al. 2004; Blake et al. 2004; Abdalla, Blake & Rawlings 2010; Power, Baugh & Lacey 2010; Kim et al. 2011).

Future galaxy surveys on the SKA and its pathfinders are expected to revolutionize our view of the H I Universe and so it is timely to ask precisely what these surveys can teach us about the physical processes that drive galaxy formation. In this paper we focus on feedback – from stars in the form of winds driven by SNe, from accreting supermassive black holes in the form of active galactic nuclei (AGN) heating and from a photoionizing background in the early Universe – and evaluate how the global properties of H I in galaxies such as the H I mass function, which quantifies the number density of galaxies of a given H I mass, and the two-point correlation function and halo occupation distributions (HODs; e.g. Kim et al. 2011), which quantify spatial clustering, are shaped by different sources of feedback.

In galaxy formation models, the strengths of these processes and the interplay between them have been traditionally set by examining the predictions of the galaxy luminosity function in the b_J band, so we will also study how this statistic changes. To do this, we use the version of the semi-analytical galaxy formation model GALFORM of Cole et al. (2000) as it has been developed by Lagos et al. (2011a); this calculates self-consistently the H I properties of galaxies by splitting their interstellar media (ISM) into H I and H_2 phases using the empirical relations of Blitz & Rosolowsky (2006) and Leroy et al. (2008), and links star formation (SF) in galaxies not to their cold gas masses, as assumed in previous models (cf. Cole et al. 2000; Baugh 2006), but to their H_2 masses, as suggested by recent observations (e.g. Bigiel et al. 2008). As shown in Lagos et al. (2011b), this model reproduces the observed H I mass function at $z = 0$, accurately reproducing its amplitude and shape at intermediate and low H I masses.

This is particularly interesting because we expect feedback to influence the global properties of galaxies selected either by their stellar mass or light. Previous studies have shown that SNe are pivotal in fixing the amplitude and slope of the luminosity function (e.g. Cole et al. 2000; Benson et al. 2003), while AGN heating suppresses the formation of massive galaxies and dictates the form of the bright end (cf. Bower et al. 2006; Croton et al. 2006). In contrast, the influence of SNe and AGN on the H I mass function (HIMF) appears more subtle. For example, Power et al. (2010) found that galaxy formation models that included or excluded AGN heating (such as De Lucia & Blaizot 2007 and Baugh et al. 2005, respectively) predict H I mass functions that reproduce equally well the observed $z \simeq 0$ data. The H I mass function offers the possibility of placing stronger constraints on the strength of feedback in semi-analytical models, which previously used only the optical properties of galaxies (e.g. Benson et al. 2003; Bower et al. 2010). At the same time, the variation of clustering strength with galaxy properties provides us with important clues about the physics of galaxy formation. Any discrepancy between observational measurements of clustering and the predictions of galaxy formation models indicates the need to improve the models, either by refining the modelling of the physical processes included or by considering the addition of further effects (see e.g. Kim et al. 2009).

The structure of the paper is as follows. In Section 2, we provide a brief overview of the Lagos et al. (2011a) model and describe how the different modes of feedback (SNe, AGN and photoionization) are implemented in GALFORM. In Section 3 we show how the different forms of feedback influence both the galaxy luminosity function in b_J band and the H I mass function, and we deduce using likelihood maximization precisely what information we glean from them. In Section 4 we investigate how the spatial clustering of H I-poor and H I-rich galaxies is influenced by feedback by inspecting the two-point correlation function and HODs. Finally, in Section 5, we summarize our results and discuss their implications for testing the modelling of feedback with forthcoming H I surveys.

2 MODELLING

In this section we first briefly give an overview of the version of GALFORM used in this paper (Section 2.1). Because the focus of our paper is on the impact of feedback on the large-scale H I properties of galaxies, we summarize the modes of feedback that are implemented in GALFORM – from SNe (Section 2.2), AGN (Section 2.3) and photoionization after cosmological reionization (Section 2.4).

2.1 The GALFORM galaxy formation model

We use the version of GALFORM (cf. Cole et al. 2000) that is described in Lagos et al. (2011a,b) to predict the properties of galaxies forming and evolving in the Λ cold dark matter cosmology adopted for the Millennium Simulation (cf. Springel et al. 2005).[1] GALFORM models the key physical processes of galaxy formation, including the gravitationally driven assembly of dark matter haloes, radiative cooling of gas and its collapse to form centrifugally supported discs, SF, and feedback from SNe and AGN.

Lagos et al. (2011a) extended GALFORM by modelling the splitting of cold gas in the ISM into its H I and H_2 components and by linking explicitly SF to the amount of H_2 present in a galaxy. Lagos et al. (2011b) compared the model predictions obtained using empirically and theoretically derived SF laws (cf. Blitz & Rosolowsky 2006; Krumholz, McKee & Tumlinson 2009) with a variety of observations (e.g. the H I mass function, ^{12}CO (1–0) luminosity function, and correlations between the ratio H_2/H I and stellar and cold gas masses) and found that the empirical law of Blitz & Rosolowsky (2006) (see also Leroy et al. 2008) is favoured by these data. This law is of the form

$$\Sigma_{\rm SFR} = \nu_{\rm SF}\, f_{\rm mol}\, \Sigma_{\rm gas}, \quad (1)$$

where $\Sigma_{\rm SFR}$ and $\Sigma_{\rm gas}$ are the surface densities of the star formation rate (SFR) and total cold gas mass respectively, $\nu_{\rm SF}$ is the inverse of the SF time-scale for the molecular gas and $f_{\rm mol} = \Sigma_{\rm mol}/\Sigma_{\rm gas}$ is the molecular-to-total gas mass surface density ratio. Importantly for the work we present in this paper, Lagos et al. (2011b) showed that the Blitz & Rosolowsky (2006) law is able to reproduce the H I mass function at $z = 0$ at intermediate and low H I masses. This is because it suppresses SF in lower mass galaxies, thereby reducing SN feedback and allowing these galaxies to retain larger gas reservoirs. Note that we use the Lagos et al. (2011b) as the default model in this paper.

[1] Recall that the cosmological parameters adopted for the Millennium Simulation are the total matter density $\Omega_{\rm M} = 0.25$, the baryon density $\Omega_{\rm b} = 0.045$, the vacuum energy density $\Omega_\Lambda = 0.75$, the Hubble parameter $H_0 = 100\,h\,{\rm km\,s^{-1}\,Mpc^{-1}}$ with $h = 0.73$, the primordial scalar spectral index $n_{\rm s} = 1$ and the fluctuation amplitude $\sigma_8 = 0.9$.

2.2 Supernova feedback

SNe act to reheat cold gas and eject it from the galaxy disc at a rate

$$\dot{M}_{\rm eject} = \beta\psi, \tag{2}$$

where ψ is the instantaneous SFR and β regulates feedback efficiency,

$$\beta = (V_{\rm disc}/V_{\rm hot})^{-\alpha_{\rm hot}}. \tag{3}$$

Here $V_{\rm hot}$ and $\alpha_{\rm hot}$ are adjustable parameters that govern the strength of the SN feedback (cf. Cole et al. 2000) and $V_{\rm disc}$ is the circular velocity of the galactic disc; the values in the default Lagos et al. (2011b) model are $V_{\rm hot} = 485$ km s^{-1} and $\alpha_{\rm hot} = 3.2$. We expect SN feedback to be most effective in low-mass dark matter haloes because gas is expelled efficiently from their shallow potential wells. From equation (3), the mass loading of the SN wind is largest in such haloes and this suppresses the formation of faint, low-mass galaxies and ensures that the faint end of the galaxy luminosity function is recovered by GALFORM, in good agreement with observational estimates (e.g. Blanton et al. 2001; Norberg et al. 2002).

2.3 AGN feedback

SN feedback is less effective in large circular velocity haloes (according to equation 3). The gas ejected from low-mass haloes can potentially cool and turn into stars in more massive haloes, generally leading to the formation of too many massive galaxies. In the absence of strong feedback in massive dark matter haloes, GALFORM predicts an overabundance of bright galaxies and a galaxy luminosity function whose bright end slope is too steep (cf. Benson et al. 2003). For this reason, Bower et al. (2006) extended GALFORM to include AGN feedback, which suppresses cooling flows in massive haloes. Physically this occurs because AGN are fuelled by supermassive black holes that grow by luminous accretion.

In GALFORM AGN feedback is modelled by assuming that the hot gaseous atmospheres surrounding massive galaxies are in quasi-hydrostatic equilibrium when the cooling time at the cooling radius, $t_{\rm cool}(r_{\rm cool})$, exceeds a multiple of the free-fall time at the cooling radius, $t_{\rm ff}(r_{\rm cool})$, i.e.

$$t_{\rm cool}(r_{\rm cool}) > \frac{1}{\alpha_{\rm cool}} t_{\rm ff}(r_{\rm cool}), \tag{4}$$

where $\alpha_{\rm cool}$ is a free parameter that regulates the strength of AGN feedback;[2] increasing $\alpha_{\rm cool}$ means that AGN feedback becomes effective in lower mass dark matter haloes. We adopt a value of $\alpha_{\rm cool} = 0.58$, which is the default in the Lagos et al. (2011b) model. We define the cooling time at halocentric radius r as

$$t_{\rm cool}(r) = \frac{3}{2}\frac{\bar{\mu} m_{\rm p} k_{\rm B} T_{\rm gas}}{\rho_{\rm gas}(r)\Lambda(T_{\rm gas}, Z_{\rm gas})}, \tag{5}$$

where $\rho_{\rm gas}$, $T_{\rm gas}$ and $Z_{\rm gas}$ are the gas density, temperature and metallicity, respectively, Λ is the cooling function,[3] $\bar{\mu}$ is the mean molecular weight, $m_{\rm p}$ the proton mass and $k_{\rm B}$ is Boltzmann's constant. We define the free-fall time at halocentric radius r by

$$t_{\rm ff}(r) = \int_0^r \left[\int_r^y -\frac{2GM(x)}{x^2}\,{\rm d}x\right]^{-1/2} {\rm d}y, \tag{6}$$

where $M(r)$ is the total mass (baryonic and dark matter) interior to r. The cooling radius, $r_{\rm cool}$, is the radius at which $t_{\rm cool}$ matches the age of the halo, which is obtained from the halo merger history.

We note that the model predicts that generally black holes gain most of their mass by accretion of gas driven to the centre of the galaxy via disc instabilities (cf. Fanidakis et al. 2011). Accretion of gas that cools from the hot atmosphere is relatively unimportant until late times, when the growth rate of the black hole scales as $L_{\rm cool}/c^2$, where $L_{\rm cool}$ is the luminosity of the cooling gas and c is the speed of light.

2.4 Photoionization feedback

Photoionization is predicted to have a dramatic impact on SF in low-mass galaxies. This is because the presence of a photoionizing background both modifies the net cooling rate of gas in haloes by removing the 'hydrogen peak' in the cooling curve (cf. fig. 1 of Benson et al. 2002) and increases the temperature of the intergalactic medium (IGM) such that its thermal pressure prevents gravitational collapse of baryons on to low-mass haloes (e.g. Efstathiou 1992; Okamoto, Gao & Theuns 2008). As a result, only those low-mass haloes that contained cold gas prior to re-ionization can form stars (e.g. Hoeft et al. 2006). GALFORM includes the Benson et al. (2002) prescription for suppressing the cooling of halo gas on to the galaxy – this occurs if the host halo's circular velocity $V_{\rm circ}$ lies below a threshold $V_{\rm cut}$ at redshift $z < z_{\rm cut}$. The values in the default Lagos et al. (2011b) model are $V_{\rm cut} = 30$ km s^{-1} and $z_{\rm cut} = 10$. The default $V_{\rm cut}$ is in good agreement with the results of hydrodynamical simulations by Hoeft et al. (2006) and Okamoto et al. (2008).

3 THE GALAXY LUMINOSITY FUNCTION AND H I MASS FUNCTION

In this section we investigate how the galaxy luminosity function in $b_{\rm J}$ band and the H I mass function at $z = 0$ are influenced by feedback from SNe, AGN and a photoionizing background. We use Monte Carlo halo merger trees generated using the algorithm described in Parkinson, Cole & Helly (2008) to predict galaxy properties. The Monte Carlo trees are tuned to match N-body merger trees extracted from the Millennium Simulation. Note that we express H I masses in units of $h^{-2}\,{\rm M}_\odot$ rather than $h^{-1}\,{\rm M}_\odot$, the mass unit used in simulations. This ensures that the observational units (which depend upon the square of the luminosity distance) are matched, but it introduces an explicit dependence on the dimensionless Hubble parameter, for which we assume the value of $h = 0.73$ used in the Millennium Simulation. We refer the reader to section 2.1 of Lagos et al. (2011b) for further discussion of this approach.

Intuitively, we expect SN feedback to be particularly damaging in low-mass galaxies because gas is expelled easily from their shallow potential wells and so SF is shut down. In contrast, SN feedback is ineffective in high-mass galaxies, which reside at the centres of massive dark matter haloes with deep potential wells; here a far more energetic source of feedback, namely AGN heating, is required, which acts to suppress the formation of very massive bright galaxies. The photoionizing background suppresses the collapse of gas on to low-mass dark matter haloes, thereby preventing galaxies from forming. The influence of these distinct processes on the galaxy luminosity function is straightforward to predict – photoionization and SN feedback will govern the amplitude and shape of the faint end, while AGN heating dictates the amplitude and shape of the bright end. Predicting their impact on the H I mass function is less

[2] We note that equation (2) of Bower et al. (2006) contains a typographical error.

[3] We use the tabulated cooling functions of Sutherland & Dopita (1993).

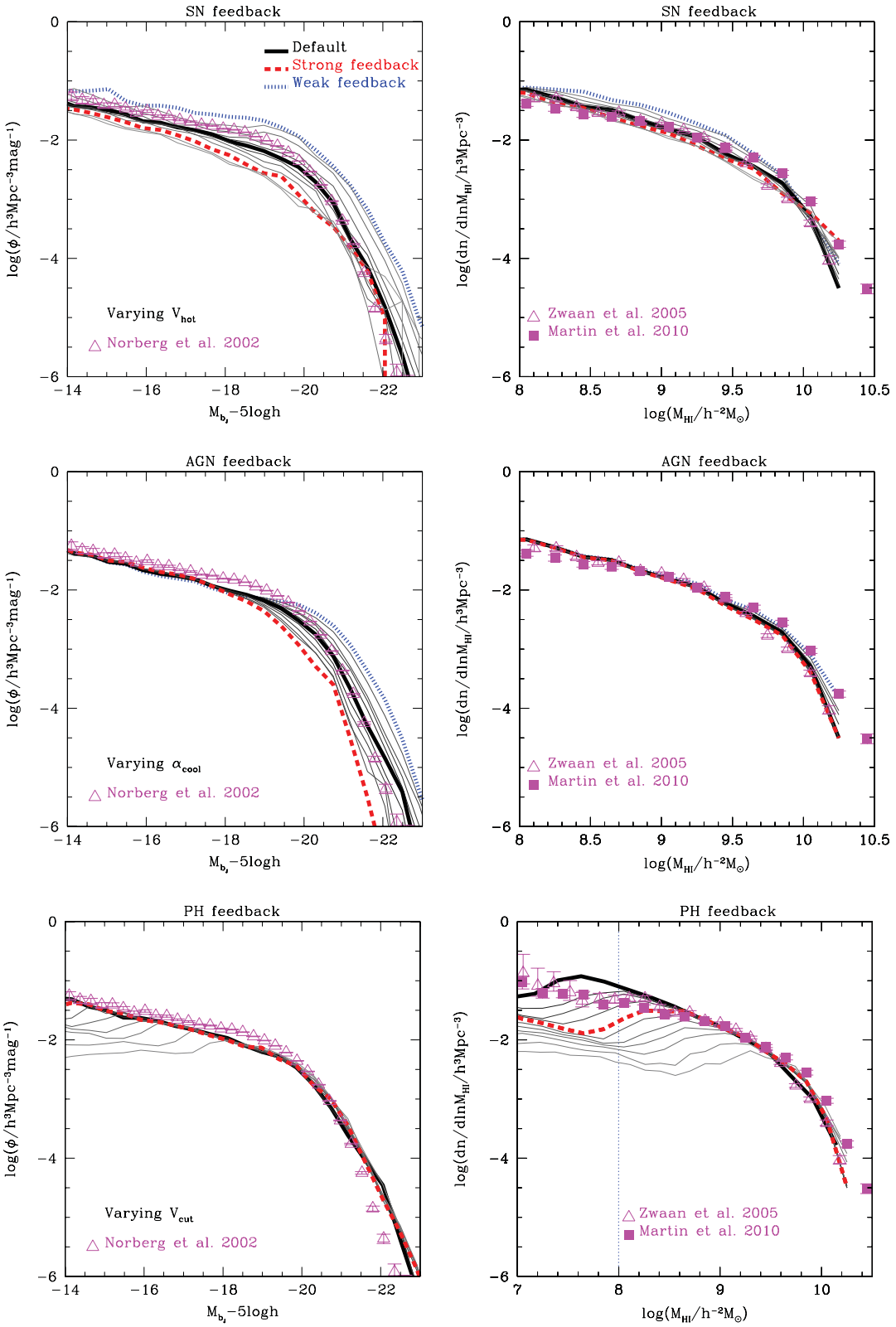

Figure 1. Impact of feedback from SNe, AGN and a photoionizing background (top, middle and bottom rows) on the predicted b_J-band galaxy luminosity function (left-hand panels) and H I mass function (right-hand panels); symbols correspond to data from the 2dF Galaxy Redshift Survey (open triangles; cf. fig. 11 and table 1 of Norberg et al. 2002), HIPASS (open triangles; cf. Zwaan et al. 2005) and ALFALFA (filled squares; cf. Martin et al. 2010). SN strength varies in the range of $300 \leq V_{\rm hot} \leq 700\,{\rm km\,s^{-1}}$, assuming fixed $\alpha_{\rm hot}$; AGN strength in the range of $0.4 \leq \alpha_{\rm cool} \leq 0.8$; and photoionization strength in the range of $30 \leq V_{\rm cut} \leq 90\,{\rm km\,s^{-1}}$. The darker the line, the closer the strength of the feedback parameter to its default value. Red dashed and blue dotted curves correspond to models with strong and weak feedback; the dotted vertical line in the lower right-hand panel indicates the lower H I mass limit in the galaxy formation model we use them as reference models in Section 4.

straightforward – as noted in Lagos et al. (2011b), the most H I-rich galaxies are likely to be low-mass systems, in which case the imprint of SN feedback may span the mass function, whereas the influence of AGN heating may be negligible.

We investigate these ideas in Fig. 1, in which we explore the impact of SN-driven winds (upper panels), AGN heating (middle panels) and a photoionizing background (lower panels) on the galaxy luminosity function in b_J band (left-hand panels) and H I mass function (right-hand panels) at $z = 0$. For comparison we plot the b_J-band galaxy luminosity function (open triangles) estimated from the 2 degree Field Galaxy Redshift Survey (2dFGRS) by Norberg et al. (2002) in the left-hand panels, and the H I mass functions deduced from the HIPASS (open triangles) and ALFALFA (filled squares) surveys by Zwaan et al. (2005) and Martin et al. (2010), respectively.

Impact of SN feedback. We vary the parameter $V_{\rm hot}$, which governs the mass ejection rate, $\dot{M}_{\rm eject}$, assuming a fixed value of $\alpha_{\rm hot}$, between 300 km s^{-1} (less effective) and 700 km s^{-1} (more effective); recall its default value is 485 km s^{-1}. By varying $V_{\rm hot}$ we are in essence changing the mass of the system in which SN feedback is effective. On the other hand, varying $\alpha_{\rm hot}$ would result in the same galaxies being affected by SNe, but with different mass loading in the winds of reheated material. The upper panels indicate that varying $V_{\rm hot}$ in this way leads to systematic and measurable offsets in both the luminosity function and H I mass function – stronger (weaker) SN feedback decreases (increases) the number of galaxies of a given luminosity (by $\sim$0.5–1 dex) or H I mass (by $\sim$0.5 dex). Interestingly, weaker feedback leaves the shape of the luminosity and H I mass functions broadly unaffected, whereas stronger feedback leads to slightly steeper slopes at the faint/low-mass and bright/high-mass ends. Red dashed and blue dotted curves correspond to models with strong (600 km s^{-1}) and weak (300 km s^{-1}) feedback; we use these as reference models in Section 4, where we examine the clustering of H I-rich and H I-poor galaxies.

Impact of AGN feedback. Here we vary the parameter $\alpha_{\rm cool}$ in the range of $0.4 \leq \alpha_{\rm cool} \leq 0.8$; recall its fiducial value is $\alpha_{\rm cool} = 0.58$. Increasing $\alpha_{\rm cool}$ decreases the halo mass at which AGN heating starts to become effective. The middle panels of Fig. 1 demonstrate that AGN heating has little influence beyond the bright end of the galaxy luminosity function or the high-mass end of the H I mass function, regulating both the sharpness of the transition between faint/bright and low-/high-mass galaxies and the position at which it occurs. The number of bright galaxies is very sensitive to the strength of AGN feedback, varying by as much as a factor of $\sim$100 for the most luminous systems. Interestingly, AGN feedback also affects the numbers of galaxies with high H I masses, but the effect is only apparent in the cases of the weakest feedback. Red dashed and blue dotted curves correspond to models with strong ($\alpha_{\rm cool} = 0.8$) and weak ($\alpha_{\rm cool} = 0.4$) AGN feedback, which, as before, we use as reference models in Section 4.

Impact of Photoionization. Two parameters, $V_{\rm cut}$ and $z_{\rm cut}$, govern photoionization in the model. We find that $z_{\rm cut}$, the redshift at which reionization occurs, has little influence on either the galaxy luminosity function or H I mass function at $z = 0$ – varying $z_{\rm cut}$ in the range of $6 \leq z_{\rm cut} \leq 12$, the range suggested by measurements of polarization in the cosmic microwave background radiation and the Gunn–Peterson effect in distant quasars (e.g. Greiner et al. 2009; Komatsu et al. 2011)produce luminosity and H I mass functions that are indistinguishable to within the line width. For this reason we concentrate on $V_{\rm cut}$, which we vary in the range of $30 \leq V_{\rm cut} \leq 90$ km s^{-1}. The minimum progenitor mass we consider is $5 \times 10^8\, h^{-1}\, {\rm M}_\odot$ to explore low $V_{\rm cut}$ values (see also H I mass function in Fig. 1 which has lower H I mass limit than other cases of H I mass function, indicated by the vertical dotted line). Increasing $V_{\rm cut}$ suppresses cooling in all haloes with circular velocities $V_{\rm cir} \leq V_{\rm cut}$ at $z < z_{\rm cut}$ and its impact is most pronounced at the faint end of the galaxy luminosity function and the low-mass end of the H I mass function. The red dashed curve corresponds to a model with strong (50 km s^{-1}) photoionization feedback, which we use as a reference model in Section 4.

Constraints on Galaxy formation models. What information can we glean from the galaxy luminosity and H I mass functions about the various modes of feedback? We investigate this using the galaxy luminosity function of Norberg et al. (2002) and the H I mass function of Zwaan et al. (2005). Although the Martin et al. (2010) ALFALFA mass function extends to lower H I masses, it has more limited sky coverage than the Zwaan et al. (2005) HIPASS mass function and so is more susceptible to the effects of cosmic variance. We quantify the constraints offered by the observational data by calculating the ratio of likelihoods $L/L_{\rm default}$ for each models with respect to default model,

$$\frac{L}{L_{\rm default}} = \frac{\Sigma|\log({\rm od}_i) - \log({\rm md}_i)|}{\Sigma|\log({\rm od}_i) - \log({\rm md}_i)|_{\rm default}}. \quad (7)$$

Here we sum over the difference in log values of the observational data ($\rm od_i$) and the predictions ($\rm md_i$) for each model and compare with the sum over this difference for the default model. Our results are plotted in Fig. 2, where solid (dotted) curves indicate how $L/L_{\rm default}$ varies with SNe, AGN and photoionization feedback strength (left-hand, middle and right-hand panels) for the galaxy luminosity function (H I mass function).

Formally, the models give a poor fit to the observational data. There are several reasons for this. First, the parameters we vary are physical, not statistical, and affect the predictions of the model in a complex way, due to the interplay between different physical processes. With a parametric functional form, such as the Schechter function, the consequences of changing a parameter are transparent. Secondly, GALFORM predicts a whole range of galaxy properties, and the luminosity function or H I mass function represents just one way of describing the population of model galaxies. The parameters of the default model were chosen as a compromise in reproducing a variety of observational data, not just the luminosity function or mass function. If we chose to fit the data considered here in isolation, with complete disregard for any other data set, it would be possible to improve the fits. Nevertheless, it is not clear that we would obtain a formally acceptable fit. Again, the reason for this is that GALFORM is a physical model rather than a parametric fitting formula. The shortcomings of the model could be encoded in a 'model discrepancy' that broadens the errors in a χ^2 fit (see Bower et al. 2010 for a more formal approach to this). Finally, the observational errors do not include all of the contributions (e.g. sample variance) and exclude systematics (e.g. the k-correction in the case of the luminosity function). The key point we aim to get across from this plot is the shape of the $L/L_{\rm default}$ curves: how rapidly do we move away from the quality of the fit in the default model on varying the parameter? If the value of $L/L_{\rm default}$ varies rapidly on comparing the model predictions to a particular data set, then that data set could in principle provide a tighter constraint on the parameter value.

We find that the galaxy luminosity function shows a strong dependence on the strength of SN feedback and a moderate dependence on the strength of AGN feedback, with a narrow range of

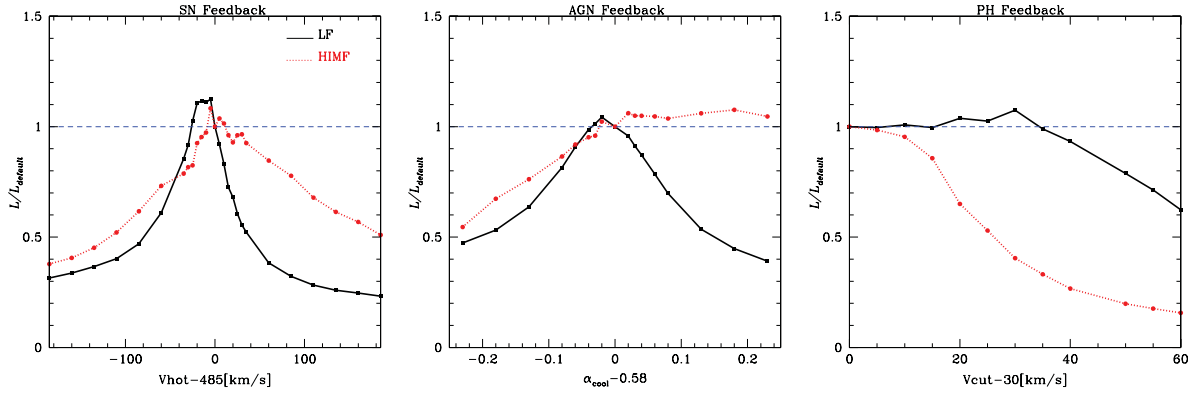

Figure 2. Values of $L/L_{\rm default}$ obtained for the SNe, AGN and photoionization feedback models (left-hand, middle and right-hand panels), where $L/L_{\rm default}$ is calculated using equation (7). Solid (dotted) curves show how $L/L_{\rm default}$ for the galaxy luminosity function in $b_{\rm J}$ band (H I mass function) as we vary systematically the SNe, AGN and photoionization strength; filled squares (circles) indicate the values for the models that have been run. For reference we also show dashed horizontal lines corresponding to $L/L_{\rm default} = 1$. See text for further details.

preferred values close to their default values; the H I mass function offers a weak constraint on SN feedback and no constraint on AGN feedback. In contrast, the H I mass function is sensitive to the strength of the photoionizing background, and indicates that values of $V_{\rm cut}$ larger than $\sim$70 km s^{-1} can be ruled out.

Smaller values of $V_{\rm cut}$ appear to have the same likelihood, but this can be understood as an artefact of the effective resolution of our merger trees. We use Monte Carlo merger trees to explore the impact of varying $V_{\rm cut}$, as this allows us to vary the mass resolution of the progenitor haloes to ensure that we can resolve the haloes which would be affected by the choice of this parameter. The minimum progenitor mass we consider is $5 \times 10^8\,h^{-1}\,{\rm M}_\odot$. We can obtain tighter constraints on the minimum value of $V_{\rm cut}$ by using Monte Carlo trees with higher effective resolution, but we defer this to a forthcoming paper. Our results suggest that the H I mass function, measured at $z = 0$, can provide an important constraint on the minimum halo mass that contributed to reionization, and complements estimates of the minimum halo mass based on high-redshift observations (e.g. Choudhury, Ferrara & Gallerani 2008; Srbinovsky & Wyithe 2010; Muñoz & Loeb 2011).

4 SPATIAL CLUSTERING OF H I IN GALAXIES

We now examine how feedback influences the spatial distribution of H I galaxies, which we quantify using the two-point correlation function and the HOD (cf. Benson et al. 2000; Peacock & Smith 2000; Berlind & Weinberg 2002). The clustering predictions for $b_{\rm J}$-band-selected samples were studied in Kim et al. (2009). The HOD gives the mean number of galaxies as a function of halo mass, assuming pre-defined selection criteria (e.g. colour, cold gas mass), and can be separated into contributions from central galaxies and their satellites. It is an output from the semi-analytical model. HODs for optically selected samples of galaxies have been studied extensively and are typically parametrized as step functions, which represent central galaxies, and power-law components, which represent satellites (e.g. Peacock & Smith 2000; Berlind & Weinberg 2002). In contrast, relatively few studies have been made of HODs for H I-selected samples of galaxies (e.g. Marín et al. 2010; Wyithe & Brown 2010; Kim et al. 2011) but they indicate that parametrizations of the kind adopted for optically selected galaxy samples need to be modified for H I-selected samples (cf. Kim et al. 2011).

Note that we use *N*-body halo merger trees drawn from the Millennium Simulation to obtain the spatial information required to study clustering. The resolution limit of the Millennium Simulation imposes a limit on the halo mass that we can reliably resolve of $10^{10}\,h^{-1}\,{\rm M}_\odot$, which in turn sets a limit of $M_{\rm HI} \sim 10^{8.5}\,h^{-2}\,{\rm M}_\odot$ on the H I mass that we can track.

In Fig. 3 we explore the impact of SN-driven winds (upper panels), AGN heating (middle panels) and photoionization (lower panels) on the two-point correlation function (left-hand panels) and the HOD (right-hand panels) at $z = 0$. In the top part of each panel we plot the relevant statistic for galaxies selected according to their high or low H I mass, while in the bottom part we plot the ratio of the statistic with respect to its value in the default model for galaxies of the same H I richness. Here we define H I-rich galaxies to have $M_{\rm HI} > 10^{9.25}\,h^{-2}\,{\rm M}_\odot$, while H I-poor galaxies have $10^{8.5} < M_{\rm HI} < 10^{9.25}\,h^{-2}\,{\rm M}_\odot$. For clarity, we concentrate on the typical weak and strong feedback models (blue and red curves, respectively) that we considered in Fig. 1. This is necessary because we expect environmental effects to become apparent when we measure clustering properties, and we wish to disentangle the effects of environment from feedback. We show also the two-point correlation function of gas-rich galaxies at $z = 0$ measured from the HIPASS survey, presented in Meyer et al. (2007), and the predictions for the two-point correlation function and the HOD in the default model, which is in good agreement with the HIPASS result.

Impact of SN feedback. The default model predicts that H I-rich galaxies (black solid curve) should be more strongly clustered than H I-poor galaxies (red dotted curve), which we show in the top left-hand panel. Here we see also that strong SN feedback has negligible impact on the clustering strength at large separations of both H I-rich and H I-poor galaxies (dot–dashed and dashed curves, respectively), but it influences the clustering strength of both H I-rich and H I-poor galaxies at separations $\lesssim 1\,h^{-1}$ Mpc (short dashed curve). Reducing the strength of SN feedback leads both H I-poor and H I-rich galaxies to cluster more strongly at small separations – $\lesssim 1(3)\,h^{-1}$ Mpc for H I-rich (H I-poor) galaxies. Fig. 3 shows that the clustering amplitude of both H I-poor and H I-rich samples becomes similar – as can be most easily seen in the lower panel, which shows the ratio of the clustering with respect to that of the corresponding H I sample in the default model. This trend can be understood by inspecting fig. 3 of Kim et al. (2011), in which the cold gas mass in galaxies is plotted against their host dark matter halo mass. Beyond the mass at which AGN heating stops cooling flows, there is a sudden break in the cold gas mass–halo mass

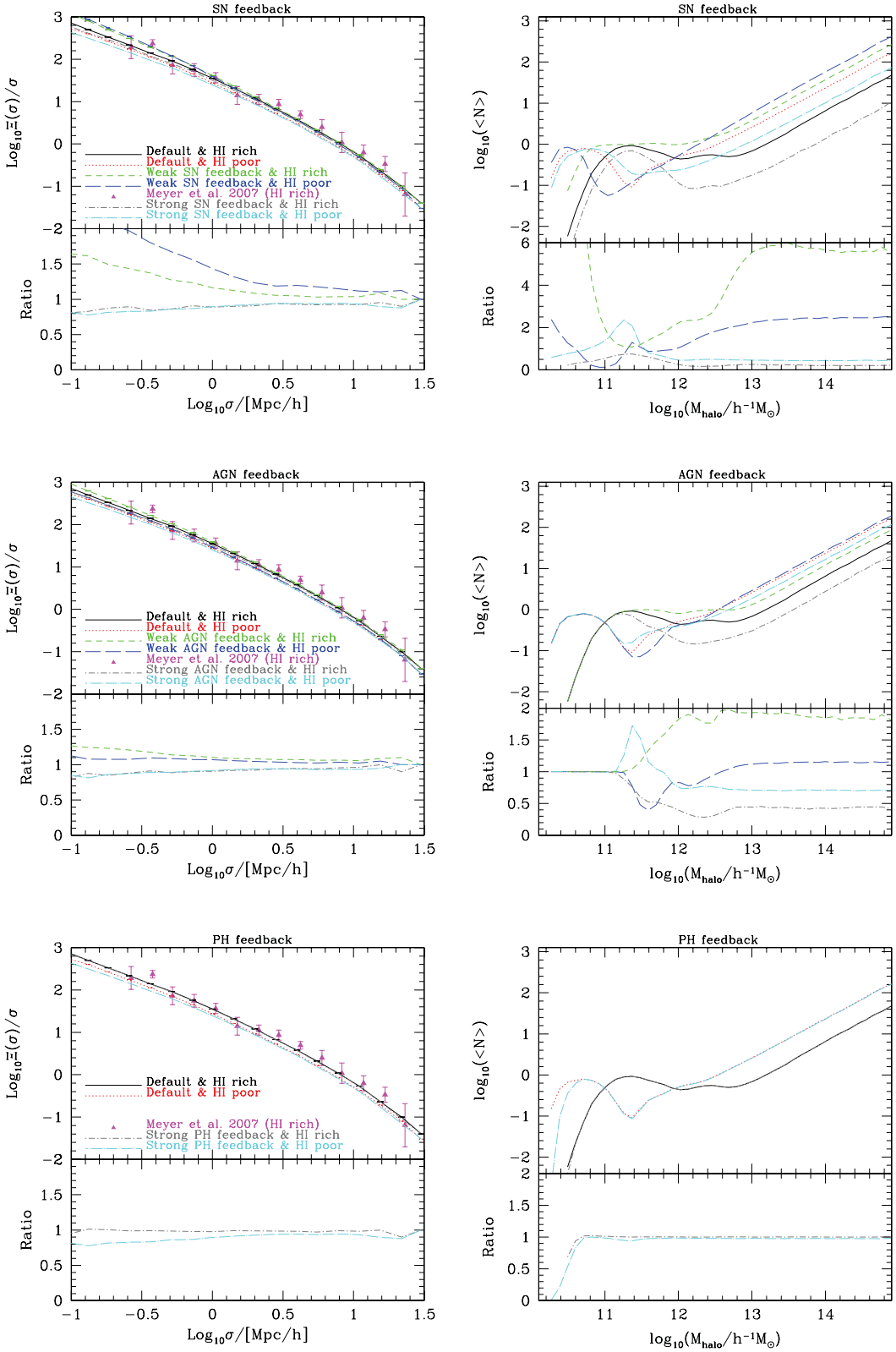

Figure 3. The impact of SNe, AGN and photoionization feedback (top, middle and bottom rows) on the two-point correlation function (left-hand panels) and the halo occupation distribution (right-hand panels). In the upper part of each panel we plot the relevant statistic for H I-poor and H I-rich galaxies, while in the lower part we plot the ratio of the H I-poor or H I-rich statistic with respect to its value in the default (H I-poor or H I-rich) model. Here H I-rich galaxies have masses $M_{\rm HI} > 10^{9.25}$ $M_{\odot}$ and H I-poor galaxies have H I masses between $10^{8.5}$ and $10^{9.25}$ $M_{\odot}$. Filled triangles show the two-point correlation function of gas-rich galaxies obtained by Meyer et al. (2007), and assorted line types refer to the different models, as indicated by the legend in the left-hand panels. See text for further details.

relation and a dramatic increase in the scatter. Above this break in mass, the presence of gas is due to accretion of haloes of lower mass, which have their own gas reservoirs, on to the main halo. By reducing the strength of SN feedback, more gas is able to stay in the cold phase in these progenitors and gas is depleted more slowly in the current host. Because there is a large scatter in galaxy cold gas mass for a given halo mass, there is a shift in the typical host mass for both H I-poor and H I-rich galaxies, leading to an increase in the clustering amplitude.

In the top right upper panel we show the predicted HODs as a function of H I richness (dashed and dotted curves) for all galaxies. Thick (thin) curves indicate strong (weak) SN feedback cases for H I-poor and H I-rich galaxies. As we would expect, stronger SN feedback leads to fewer galaxies when compared to the weaker feedback case, spanning the full range of halo masses and regardless of the H I richness of the galaxies. In the top right lower panel we plot the ratio of the number of galaxies for the strong and weak SN feedback cases compared to the default model. Again this reveals that SN feedback affects the numbers of galaxies regardless of host halo mass, but interestingly it shows that the influence of SN feedback is greater on the numbers of H I-rich galaxies compared to H I-poor galaxies.

Impact of AGN feedback. In the middle left-hand panel we show that the clustering of galaxies selected by their H I richness is largely insensitive to the strength of AGN feedback. If AGN feedback is weak, its effect on the clustering strength of H I-poor galaxies is negligible and enhances the clustering of H I-rich galaxies only at small separations. If the AGN feedback is strong, it suppresses the clustering of both H I-rich and H I-poor galaxies to a similar extent.

As before, we show in the middle right upper and lower panels the predicted HODs as a function of H I richness (dashed and dotted curves) for all galaxies, where strong (weak) AGN feedback is indicated by thick (thin) curves. The lower panel shows that AGN feedback affects haloes with masses in excess of $10^{11.2}\,h^{-1}\,\mathrm{M}_{\odot}$ and that it has a greater impact on the numbers of H I-rich galaxies than H I-poor galaxies.

Impact of photoionization. Increasing the strength of photoionization has negligible impact on the clustering strength of H I-rich galaxies, but leads to an increase in the clustering strength of H I-poor galaxies. This is because increasing the strength of photoionization corresponds to an increase in the circular velocity scale $V_{\rm cut}$ of dark matter haloes in which galaxies can form.

We show predicted HODs as a function of H I richness (dashed and dotted curves) for all galaxies in the bottom right upper and lower panels. Here we consider only the case of strong photoionization feedback because the typical halo mass affected by weak photoionization feedback ($V_{\rm cut} = 30$ km s^{-1}) drops below the resolution limit of the Millennium Simulation at early times. Thick lines indicate strong photoionization feedback, whereas thin lines show the default model for H I-poor and H I-rich galaxies. It is readily apparent that photoionization feedback has little influence over the HODs of H I-rich galaxies – the strong feedback case is indistinguishable from the default model. The lower panel shows that photoionization feedback affects only the lowest mass haloes ($10^{10.7}\,h^{-1}\,\mathrm{M}_{\odot}$) at $z = 0$.

5 SUMMARY

We have used the version of the GALFORM semi-analytical galaxy formation model (cf. Cole et al. 2000) that has been extended by Lagos et al. (2011a) to study how feedback from SNe, AGN and photoionization shapes both the galaxy luminosity and H I mass functions, and the spatial clustering of H I galaxies. The advantage of the Lagos et al. (2011a) model is that it is one of the first to predict explicitly and in a self-consistent manner how much H I should reside in a galaxy at a given time (see also Fu et al. 2010) and it has reproduced successfully the observed H I mass function at low-to-intermediate masses (cf. Lagos et al. 2011b). The main results of our study can be summarized as follows.

(i) Feedback from SNe regulates the amplitude and shape of both the galaxy luminosity function and the H I mass function. The effect is systematic, with more (less) efficient SN feedback leading to fewer (more) galaxies of a given luminosity or H I mass. It also regulates the amplitude of the two-point correlation function of H I-rich galaxies at small separations and the numbers of galaxies per halo mass as quantified by the HOD, regardless of their H I richness.

(ii) Feedback from AGN has little effect on either the faint-to-intermediate luminosity end of the galaxy luminosity function or low-to-intermediate mass end of the H I mass function – its impact is strongest for the brightest galaxies, as previous studies have argued (e.g. Bower et al. 2006; Croton et al. 2006), but it also affects the number of highest H I mass galaxies. A similar result has been reported by Fabello et al. (2011), and it also helps to explain the cold gas mass–halo mass relation presented in fig. 3 of Kim et al. (2011) for the Bower et al. (2006) model. In contrast, its impact on the clustering of H I galaxies is minor or negligible.

(iii) Feedback from photoionization is most pronounced for the faintest and most H I-poor galaxies. The redshift at which reionization occurs is not important – but the mass scale, as measured by $V_{\rm cut}$, is, and its influence is evident in both the shape and amplitude of the faint end of luminosity function and the low-mass end of the H I mass function. Our analysis suggests that the low-to-intermediate mass end of H I mass function offers the potential to constrain the models of photoionization. Interestingly, we find that the locally measured H I mass function can constrain the minimum mass of dark matter haloes that could have hosted galaxies that contributed to reionization. This complements existing studies of the high-redshift Universe that have used, for example, the electron scattering optical depth (e.g. Choudhury et al. 2008), the Lyα forest and (e.g. Srbinovsky & Wyithe 2010) and the ultraviolet luminosity function (e.g. Muñoz & Loeb 2011) to estimate the minimum halo mass. Our analysis suggests that the circular velocities of haloes in which galaxy formation was suppressed cannot be larger than $\sim$70 km s^{-1}.

(iv) Strong modes of feedback, as they are implemented in GALFORM, act to suppress the clustering strength of galaxies, regardless of their H I richness. H I-poor galaxies cluster more strongly than H I-rich galaxies if the strength of SN feedback is weakened, whereas there is little change in the clustering of either H I-rich or H I-poor galaxies if the strength of AGN feedback is weakened.

Our study suggests that forthcoming H I galaxy surveys can be most fruitfully exploited scientifically if they are part of a multiwavelength campaign. Such campaigns are being planned; for example, Deep Investigation of Neutral Gas Origins (DINGO) on ASKAP (cf. Meyer 2009) will probe the galaxy population out to $z \lesssim 0.4$ and will be combined the Galaxy And Mass Assembly (GAMA) survey (cf. Driver et al. 2011). These data sets will allow us to study not only the H I properties of galaxies that host AGN or young starbursts, but also the effects of environment and evolution with redshift.

ACKNOWLEDGMENTS

H-SK is supported by a Super-Science Fellowship from the Australian Research Council. CP thanks warmly Danail Obreschkow, Martin Meyer and Aaron Robotham for helpful discussions. This work was supported by a STFC rolling grant at Durham. The calculations for this paper were performed on the ICC Cosmology Machine, which is part of the DiRAC Facility jointly funded by the STFC, the Large Facilities Capital Fund of BIS and Durham University. Part of the research presented in this paper was undertaken as part of the Survey Simulation Pipeline (SSimPL; http://www.astronomy.swin.edu.au/SSimPL/). The Centre for All-Sky Astrophysics is an Australian Research Council Centre of Excellence, funded by grant CE11E0090.

REFERENCES

Abdalla F. B., Blake C., Rawlings S., 2010, MNRAS, 401, 743
Basilakos S., Plionis M., Kovač K., Voglis N., 2007, MNRAS, 378, 301
Baugh C. M., 2006, Rep. Progress. Phys., 69, 3101
Baugh C. M., Lacey C. G., Frenk C. S., Benson A. J., Cole S., Granato G. L., Silva L., Bressan A., 2004, New Astron. Rev., 48, 1239
Baugh C. M., Lacey C. G., Frenk C. S., Granato G. L., Silva L., Bressan A., Benson A. J., Cole S., 2005, MNRAS, 356, 1191
Benson A. J., Cole S., Frenk C. S., Baugh C. M., Lacey C. G., 2000, MNRAS, 311, 793
Benson A. J., Lacey C. G., Baugh C. M., Cole S., Frenk C. S., 2002, MNRAS, 333, 156
Benson A. J., Bower R. G., Frenk C. S., Lacey C. G., Baugh C. M., Cole S., 2003, ApJ, 599, 38
Berlind A. A., Weinberg D. H., 2002, ApJ, 575, 587
Bigiel F., Leroy A., Walter F., Brinks E., de Blok W. J. G., Madore B., Thornley M. D., 2008, AJ, 136, 2846
Blake C. A., Abdalla F. B., Bridle S. L., Rawlings S., 2004, New Astron. Rev., 48, 1063
Blanton M. R. et al., 2001, AJ, 121, 2358
Blitz L., Rosolowsky E., 2006, ApJ, 650, 933
Bower R. G., Benson A. J., Malbon R., Helly J. C., Frenk C. S., Baugh C. M., Cole S., Lacey C. G., 2006, MNRAS, 370, 645
Bower R. G., Vernon I., Goldstein M., Benson A. J., Lacey C. G., Baugh C. M., Cole S., Frenk C. S., 2010, MNRAS, 407, 2017
Choudhury T. R., Ferrara A., Gallerani S., 2008, MNRAS, 385, L58
Cole S., Lacey C. G., Baugh C. M., Frenk C. S., 2000, MNRAS, 319, 168
Croton D. J. et al., 2006, MNRAS, 365, 11
De Lucia G., Blaizot J., 2007, MNRAS, 375, 2
Driver S. P. et al., 2011, MNRAS, 413, 971
Efstathiou G., 1992, MNRAS, 256, 43
Evoli C., Salucci P., Lapi A., Danese L., 2011, ApJ, 743, 45
Fabello S., Kauffmann G., Catinella B., Giovanelli R., Haynes M. P., Heckman T. M., Schiminovich D., 2011, MNRAS, 416, 1739
Fanidakis N., Baugh C. M., Benson A. J., Bower R. G., Cole S., Done C., Frenk C. S., 2011, MNRAS, 410, 53
Fu J., Guo Q., Kauffmann G., Krumholz M. R., 2010, MNRAS, 409, 515
Giovanelli R. et al., 2005, AJ, 130, 2598
Greiner J. et al., 2009, ApJ, 693, 1610
Hoeft M., Yepes G., Gottlöber S., Springel V., 2006, MNRAS, 371, 401
Johnston S. et al., 2008, Exp. Astron., 22, 151
Jonas J., 2007, in From Planets to Dark Energy: The Modern Radio Universe. Univ. Manchester, UK
Kilborn V. A. et al., 2002, AJ, 124, 690
Kilborn V. A., Forbes D. A., Barnes D. G., Koribalski B. S., Brough S, Kern K., 2009, MNRAS, 400, 1962
Kim H.-S., Baugh C. M., Cole S., Frenk C. S., Benson A. J., 2009, MNRAS, 400, 1527
Kim H.-S., Baugh C. M., Benson A. J., Cole S., Frenk C. S., Lacey C. G., Power C., Schneider M., 2011, MNRAS, 414, 2367
Komatsu E. et al., 2011, ApJS, 192, 18
Krumholz M. R., McKee C. F., Tumlinson J., 2009, ApJ, 699, 850
Lagos C. D. P., Lacey C. G., Baugh C. M., Bower R. G., Benson A. J., 2011a, MNRAS, 416, 1566
Lagos C. D. P., Baugh C. M., Lacey C. G., Benson A. J., Kim H-S., Power C., 2011b, MNRAS, 418, 1649
Leroy A. K., Walter F., Brinks E., Bigiel F., de Blok W. J. G., Madore B., Thornley M. D., 2008, AJ, 136, 2782
Marín F. A., Gnedin N. Y., Seo H.-J., Vallinotto A., 2010, ApJ, 718, 972
Martin A. M., Papastergis E., Giovanelli R., Haynes M. P., Springob C. M., Stierwalt S., 2010, ApJ, 723, 1359
Meyer M., 2009, Panoramic Radio Astronomy: Wide-field 1-2 GHz Research on Galaxy Evolution,
Meyer M. J. et al., 2004, MNRAS, 350, 1195
Meyer M. J., Zwaan M. A., Webster R. L., Brown M. J. I., Staveley-Smith L., 2007, ApJ, 654, 702
Muñoz J. A., Loeb A., 2011, ApJ, 729, 99
Norberg P. et al., 2002, MNRAS, 336, 907
Okamoto T., Gao L., Theuns T., 2008, MNRAS, 390, 920
Parkinson H., Cole S., Helly J., 2008, MNRAS, 383, 557
Passmoor S. S., Cress C. M., Faltenbacher A., 2011, MNRAS, 412, L50
Peacock J. A., Smith R. E., 2000, MNRAS, 318, 1144
Power C., Baugh C. M., Lacey C. G., 2010, MNRAS, 406, 43
Serra P. et al., 2012, MNRAS, 422, 1835
Springel V. et al., 2005, Nat, 435, 629
Springob C. M., Haynes M. P., Giovanelli R., 2005, ApJ, 621, 215
Srbinovsky J. A., Wyithe J. S. B., 2010, Publ. Astron. Soc. Aust., 27, 110
Sutherland R. S., Dopita M. A., 1993, ApJS, 88, 253
Wyithe J. S. B., Brown M. J. I., 2010, MNRAS, 404, 876
Zwaan M. A. et al., 2003, AJ, 125, 2842
Zwaan M. A., Meyer M. J., Staveley-Smith L., Webster R. L., 2005, MNRAS, 359, L30

This paper has been typeset from a TEX/LATEX file prepared by the author.